Investigation of the wavelength accuracy of Brewer spectrophotometers

Julian Gröbner, David I. Wardle, C. Thomas McElroy, and James B. Kerr

The wavelength accuracy of the Brewer spectrophotometer in the 280–360-nm spectral range is improved by a new grating-drive mechanism and a new dispersion function derived from the Brewer geometry. With the new mechanism, the reproducibility of wavelength settings for spectral emission lines is better than 0.3 pm (0.0003 nm) and, with a thermally compensated version, the effect of temperature is less than 0.4 pm K^{-1}. The new dispersion function fits spectral line positions better than the standard function and is less prone to extrapolation error. Applying the new function to data from four new and ten standard drives shows that the new drives perform as well as the best of the standard ones and much better than the majority. © 1998 Optical Society of America

OCIS codes: 010.4950, 120.4140, 120.6200, 300.6540.

1. Introduction

In the past decade the Brewer spectrophotometer has become a *de facto* standard for routine column ozone measurements from the ground. More than 100 instruments are now deployed worldwide and routinely measure and report ozone values. Also, because of concern about the increase of solar ultraviolet (UV) radiation that is due to decreasing stratospheric ozone concentrations,[1,2] the Brewer spectrophotometer is used extensively to record spectral solar UV radiation. For both types of measurement accurate knowledge of the measurement wavelength is crucial because of the strong gradient in ozone absorption below 320 nm. Between the radiation detection threshold around 290 nm (depending on solar elevation, ozone amount, instrument sensitivity, etc.) and 320 nm, the radiation intensity changes by more than 5 orders of magnitude. Small errors in the assigned wavelength introduce large deviations in the measured solar radiation and thus in the retrieved ozone amount. Although the wavelengths used in the Brewer ozone measurement are chosen to minimize the effect of wavelength shift, an error of 0.1 nm in wavelength still causes an error of from 3 to 5% in the calculated column ozone amount.

The authors are with Atmospheric Environment Service, 4905 Dufferin Street, Downsview, Ontario M3H 5T4, Canada.

Received 1 July 1998; revised manuscript received 17 September 1998.

0003-6935/98/368352-09$15.00/0

The Brewer spectrophotometer is constructed with either one or two modified Ebert–Fastie type monochromators (single or double Brewer).[3,4] The first monochromator disperses the incoming radiation onto six exit slits. In the case of the double Brewer (DB), the six exit slits (intermediate slits) of the first monochromator are the entrance slits to a second monochromator that is used in the recombining mode. The entrance slit and the intermediate slits are approximately 0.55 nm wide. Because the final exit slit on a DB is approximately 0.80 nm wide, the spectral characteristics of the instrument are mainly determined by the dispersing monochromator. Consequently, the DB has the same generic spectral characteristics, except for stray light rejection, as the single Brewer (SB). Also, because of the wider final slit, there is a range of settings of the recombining monochromator, rather than a single correct setting, that can be tolerated for any given setting of the dispersing monochromator. Within this range, the setting of the recombining monochromator does not affect the signal.

The wavelength range of DB's and of new SB's is approximately 280–365 nm; approximately 70 nm of this is achieved by rotating the grating, and an extra 15 nm comes from using different exit slits. Most SB's have a scan range of approximately 40 nm. The drive mechanism, consisting of a motor-driven micrometer linked to an arm that rotates the grating, is essentially the same for all types. The smallest wavelength increment (one motor step) varies steadily from approximately 8.0 pm (0.0080 nm) at

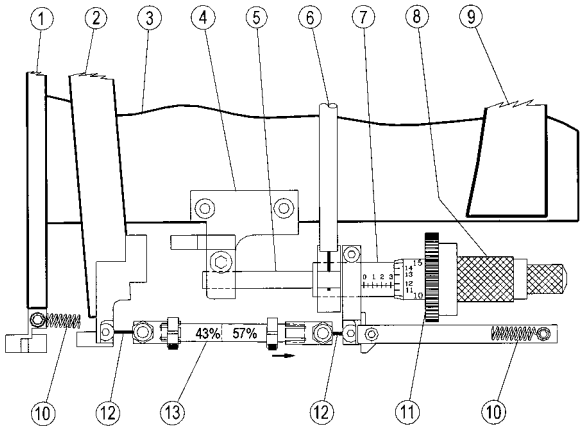

Fig. 1. New grating drive for Brewer spectrophotometers: 1, front plate of monochromator that carries the entrance and exit slits; 2, arm that rotates with the grating; 3, monochromator base plate that is normally horizontal; 4, micrometer mounting block that clamps onto the micrometer spindle; 5, spindle of the micrometer; 6, one of the two arms in the linkage that prevents rotation of 7 and is approximately 70 mm above the micrometer; 7, middle part of the micrometer; 8, thimble of the micrometer; 9, main mirror of the monochromator; 10, tension spring; 11, gear wheel mounted on the thimble; 12, wire pivots at each end of 13; 13, push-rod showing the clamps that allow easy substitutions and the 43 and 57% proportions of aluminum and Invar.

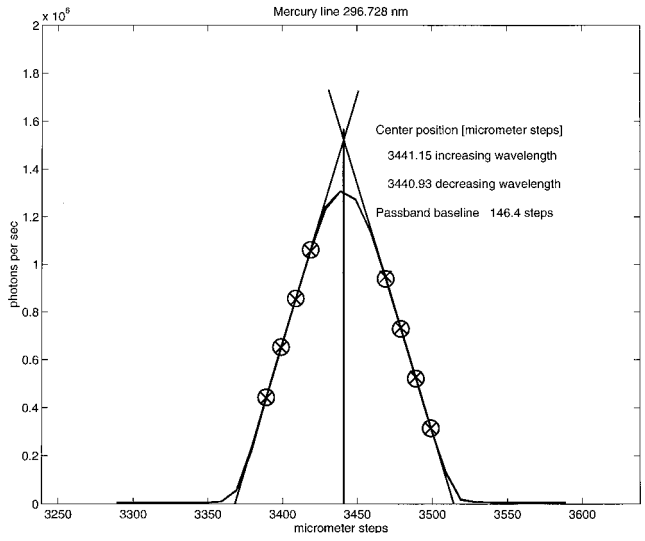

Fig. 2. Example of a 296.728-nm mercury line scan as well as the calculated center position using only the points between 20% and 80% of the maximum that are fitted to an isosceles triangle. The circles and crosses are the fitted points, respectively, for the increasing and decreasing wavelength scan.

the shorter wavelengths to 7.0 pm for the longest wavelengths.

In this paper we present the results of an investigation of a new grating drive mechanism in which the most important innovation is the link or push rod between the grating arm and the micrometer. The original push rod was 40 mm long and 6 mm in diameter with cube-corner indentations at either end fitting a small sphere fixed to the grating arm and the spherical tip of a conically shaped micrometer spindle. In many Brewers, the cube-corner indentation at the micrometer end has been replaced by a miniature bearing with five balls in a spherical cup. The new push rod, which is the same size as the original, is attached at either end by short lengths of wire that act as pivot points allowing the necessary flexibilities while preserving longitudinal rigidity. The mounting of the micrometer, which is of the nonrotating type, and modifications to it are described in Appendix A and shown in Fig. 1. The intention of the new design was to minimize friction (and the consequent hysteresis), variability, and wear by eliminating rolling or rubbing contacts in the linkage from the micrometer to the grating. This was done using the wire pivots. The cross-wire grating axle, which has always been in Brewer spectrometers, is frictionless. Consequently the only sources of friction associated with setting the rotation of the grating in the new design are in the micrometer, the motor, and the gears between them.

In a previous study,[5] aspects of the stability and reproducibility of this new grating drive were inferred from measurements obtained by moving the micrometers of the dispersing and recombining monochromators separately. The radiation source was a quartz halogen lamp that emits a continuous spectrum. Here the analysis is of measurements that were made on spectral lamps and, primarily, about the motion of the micrometer of the dispersing monochromator. This removes some of the uncertainties in the previous study in which only differences between the two micrometer movements were analyzed.

In Sections 2, 3, and 4 we discuss the spectral measurements and their associated accuracy and stability versus time and temperature obtained on the same DB (119) that was used in the previous study. In Sections 5 and 6 we describe a new dispersion calculation unique to the Brewer spectrophotometer that improves the wavelength-setting accuracy in comparison with the present method. This analysis is not restricted to use of the new grating drive and was successfully applied to a variety of SB and DB's. In addition, the amplitudes of the periodicities associated with the micrometer drive can be examined with this new dispersion calculation.

2. Spectral Line Measurements

All the data in this study are derived from recording the signals from low-pressure spectral discharge lamps while the grating drive is adjusted to scan across the emission lines. Figure 2 is an example of such a spectral scan, the horizontal axis being the number of motor steps measured from a reference position. Here, as in the standard Brewer dispersion software, each spectral scan is fitted with an isosceles triangle determined from all the points with intensities between 20% and 80% of the maximum. The scan increment is normally 10 steps which yields from 6 to 8 points for the analysis. The peak of the

isosceles triangle is taken to define a motor step number, not usually an integer, that represents the scan or wavelength. Thus each scan results in a wavelength/step number pair. The dispersion function, which is the needed relationship between wavelength and step number, is usually obtained by fitting a polynomial in step number to as many of the wavelength/step number pairs as are available. The first derivative of the dispersion function, also called the dispersion, is typically 7.5 pm step^{-1} for the Brewer. It is common practice to derive the spectral sampling function, often called the slit function, from a spectral line scan such as in Fig. 2. This can be done by multiplying the horizontal scale by the negative dispersion and shifting the resulting wavelength scale so that the triangle peak occurs at the wavelength of the lamp radiation, 296.728 nm in this case. The result describes the response when the wavelength of the incident radiation is changed and the wavelength setting (i.e., step number) of the spectrometer is fixed. Similarly the reproducibility of the wavelength setting can be inferred from the spread of motor step numbers obtained from repeated scans of the same line. Specifically, if the spectrometer had been measuring at a fixed wavelength setting in the conditions when the line scans were made, it would have recorded the irradiance with sampling functions that were shifted in wavelength within the range given by the product of the step number range and the dispersion. In what follows, the stability and temperature dependence of the wavelength settings are assessed with this rationale from repeated scans of the same spectral lines.

With regard to Fig. 2, DB 119 being a double spectrophotometer, the micrometer in the recombining monochromator is necessarily being moved in synchronism with that in the dispersing monochromator. The movement is within the above-mentioned range of tolerance, typically ± 10 steps, so the line profile is determined by the dispersing monochromator. The text on Figure 2 shows that the results from the upward and downward scans are different by 0.23 steps, although the points plotted for the two scans are not distinguishable. This backlash is typical of the old and new drive mechanisms. Backlash has been less than 0.5 steps in all the several thousand scans that were examined on the four new tested drive mechanisms. The means of the upward and downward scan results are used for the analysis.

3. Wavelength Stability versus Temperature

Although most Brewer spectrophotometers are fitted with thermally activated heaters to keep the instrument temperature above 0 °C, there is no other thermal regulation, and the temperature often fluctuates by more than 20 °C throughout the day. This necessitates that the dispersion function be checked and adjusted many times per day, which is done by the Hg routine. The routine finds the motor step number corresponding to a mercury (Hg) line, now 296.728 nm and offsets the function so that it correctly indicates the 296.728-nm position. In this section we describe a test on DB 119 with the new drive mechanism in which the Hg lines at 296.728 nm (297 nm) and 334.148 nm (334 nm) are alternately scanned for many hours and their step number positions are recorded without any resetting. The measurements were taken over a range of temperatures (i.e., 2–27 °C) by starting the tests indoors and then taking the instrument outside and continuing the measurements while it cooled. The purpose was to characterize the stability and possibly improve it so that the frequency of calling the Hg routine and the consequent loss of observation time might be reduced.

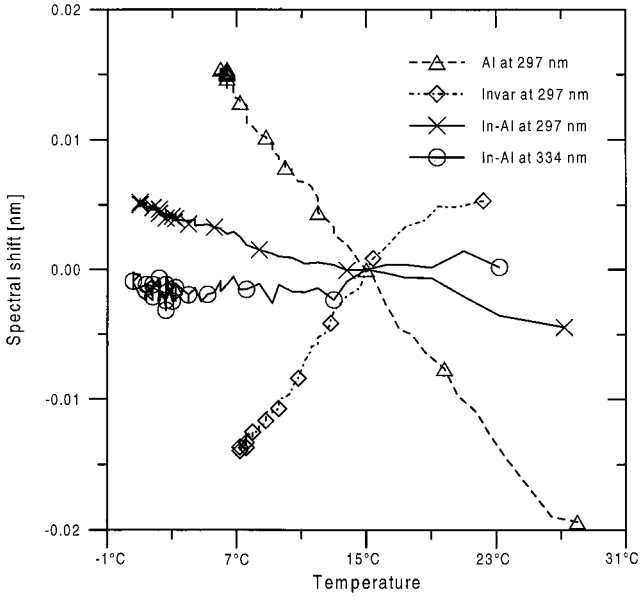

Fig. 3. Spectral line measurements of the 296.728-nm mercury line for different temperatures and different push rod materials. The circles represent measurements of the 334.148-nm mercury line with the composite push rod (43% aluminum, 57% Invar) performed alternately with measurements of the 296.728-nm mercury line. In this plot, there is one symbol for every seven data points. All the measurements were obtained for decreasing temperatures.

The test was first performed with an aluminum push rod and then with one made of Invar. It was expected that these tests would have different results because the push rod links the micrometer to the grating, and any thermal expansion in the push rod will cause the grating to rotate. The results for the 297-nm line are shown in Fig. 3 in which the step numbers are converted into wavelength shift. As can be seen, with aluminum, the wavelength setting increases by 0.035 nm when the instrument cools by 25 °C (i.e., 1.4 pm K^{-1}) whereas the change for the Invar rod is in the opposite direction and of approximately the same magnitude. These two plots also suggest, by their curvature, that the temperature sensor is initially being cooled faster than the body of the spectrometer. For this reason the temperature coefficients are estimated from the start and end points only. Based on these results a composite rod with 57% of its length Invar and 43% aluminum should produce near-zero temperature dependence.

Such a push rod was fabricated and tested; the measured temperature dependencies are -0.4 pm K^{-1} at 297 nm and $+0.1$ pm K^{-1} at 334 nm, both shown in Fig. 3. This is more than three times better than with the aluminum push rod. The small difference at the two wavelengths, or spectrum stretching, means that temperature dependence can be suppressed only at one wavelength by this method. The coefficient of spectrum stretching is 1.2×10^{-5} K^{-1}, and we believe it would be the same for any push rod composition and that it applies over the full spectral range. This implies that the temperature dependence at 360 nm would be $+0.4$ pm K^{-1} and that wavelength settings change by 8 pm or less over the full wavelength range for a temperature change of 20 °C. For comparison, a test on a DB equipped with the standard wavelength drive and push rod gave a temperature dependence of 1.6 pm K^{-1} and a stretching of 2.0×10^{-5} K^{-1}.

4. Wavelength Reproducibility

The reproducibility of wavelength settings corresponding to the two spectral lines is indicated by the scatter of the points about the smoothed fits (not shown) to each of the curves in Fig. 3. In particular, for 297 nm, the average rms scatter about the linear fits for temperatures below 15 °C is 0.038 steps, i.e., 0.3 pm, and the largest single deviations from these linear fits are approximately 0.1 steps or 0.75 pm. It should be noted that the 297- and 334-nm spectral lines were measured alternately, thus rotating the grating by a large amount between successive measurements of the same spectral line. Reproducibility obtained by taking the standard deviation of a series of measurements made at a steady temperature is typically 0.03 steps. The scatter about the 334-nm line is much larger, approximately 0.10 steps rms, because of the photon noise affecting the result of the finding algorithm for this weak line. In contrast, the photon noise in finding the 297-nm step position is only approximately 0.01 steps, which means that virtually all the above 0.03-step rms scatter must be attributed to the drive mechanism.

5. Dispersion Function

Mercury, cadmium, indium, and zinc spectral discharge lamps have lines that are suitable for wavelength calibration in the Brewer spectral range of 280–365 nm. The basic data for wavelength calibration are a set of wavelength/step number pairs obtained from line scans of these lamps, preferably by the isosceles triangle method, for as many slits and wavelengths as are available. However, lines that have overlapping peaks should not be used because the overlap prevents an accurate finding of the positions. The standard Brewer wavelength calibration has been to establish a separate dispersion function for each slit by fitting the available data for that slit with a quadratic in step number. This procedure has some definite inadequacies, which were not evident for the original 290–325-nm range, and that are in large measure due to the limited number of available spectral lines. Specifically,

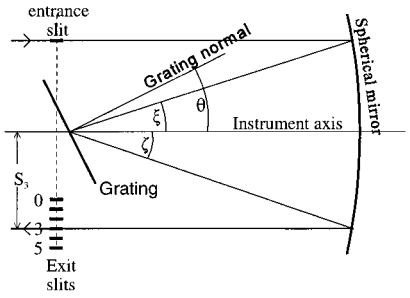

Fig. 4. Schematic view of the dispersive Brewer monochromator showing the instrument axis without the coma-correcting lens. The relevant dimensions are given in Table 1.

- Because all slits are analyzed independently, a total of 18 (6 slits times 3 coefficients) parameters must be determined. It is obvious that these parameters are related because, for example, they all describe the micrometer movement.
- A quadratic polynomial may not be adequate to express the dispersion over the full spectral range as has been shown for at least one instrument[6] and as is shown here.
- A separate analysis of each slit leaves large gaps between spectral lines where the smoothness of the grating drive has to be assumed. Also, depending on what spectral lines are available, there may be errors of extrapolation at either end of the spectral range.
- Errors up to 0.10 nm have been identified at the longer wavelengths by comparing UV observations with extraterrestrial spectra.[7]

A new method of deriving dispersion functions, which mitigates these problems, is described here. It takes account of the Brewer geometry and projects measurements from all slits onto one reference slit. A single polynomial is fitted to the whole data set to obtain an expression relating the micrometer steps to the wavelength measured at or projected onto the reference slit. Wavelengths for the other slits can then be calculated using the grating equation and the known slit positions. In the following discussion, slit 3 was chosen as the reference slit.

The method is based on the grating equation with the angles of the grating normal θ and of the incident and diffracted rays ξ and ζ, all measured from the instrument axis as shown in Fig. 4. The six diffraction angles ζ_i corresponding to the exit slits are related to the distances S_i from the individual slits to the instrument axis by

$$\sin\frac{\zeta_i}{2} = \frac{S_i}{R}, \tag{1}$$

Table 1. Brewer Design Statistics in Millimeters[a]

Mirror radius	324
Line density (n/d) of grating (mm^{-1})	3600
Entrance slit–slit 3 separation	107.91
Entrance slit–Instrument axis	50.01
Slit 0*–Slit 3	−11.116
Slit 0–Slit 3	−10.122
Slit 1	−7.158
Slit 2	−3.485
Slit 4	3.434
Slit 5	6.871

[a]The quoted uncertainties from the technical drawings for the individual slit positions are ±0.013 mm. On older instruments, slit 0 was at a different position, denoted by slit 0*.

where R is the mirror radius. The angle ξ and the entrance slit position are related in the same way. The grating equation, in terms of these angles, is

$$d[\sin(\theta - \xi) + \sin(\theta + \zeta)] = n\lambda_i, \quad (2)$$

where d and n are, respectively, the grating line frequency and the order of diffraction and λ_i is the center wavelength passing through slit i. It follows from Eq. (2) that λ^P, the center wavelength passing through slit 3, can be expressed as

$$\lambda^P = \frac{d}{n}[\sin(\theta + \zeta_3) + \sin(\theta - \xi)]. \quad (3)$$

The procedure starts with calculating the angles ξ and ζ_i from the slit positions using Eq. (1) and the dimensions of the Brewer as given in Table 1. Next, for every measurement not on slit 3, the grating angle θ is calculated from the wavelength using Eq. (2). The wavelength λ^P is then calculated using Eq. (3), and a new wavelength/step number pair is formed by replacing the lamp wavelength with λ^P, keeping the original step number. The new pair is considered to be projected onto slit 3. The dispersion function is derived by fitting a polynomial in step number to all the pairs, whether projected onto slit 3 or measured there. The polynomial degree can be chosen so as to optimize the quality of the final fit. In this study, most of the results are from our using third- or fifth-order polynomial fitting.

This first derivation of the dispersion function is not accurate because of factors ignored in the simple model of the Brewer represented by Eq. (1). For example, no account is taken of the coma-correcting lens or the effects of small but otherwise tolerable misalignments. We found that these effects can be accommodated to a good accuracy by allowing the model positions of slits 0, 1, 2, 4, and 5 to vary (keeping slit 3 fixed), which is needed in any case because the manufacturing tolerance on the slit positions (±13 μm) translates to a wavelength uncertainty much larger than what is achieved by the dispersion analysis.

The required slit positions are found iteratively. After every derivation of the dispersion function, the residuals Δ_i are grouped according to the original slits from which the pairs were projected. Slit adjustments δS_i are then calculated from the averages Δ_i of these groups by dividing by the dispersion at the slits, for which the nominal value, 1.0 nm mm^{-1}, is sufficiently accurate. The adjustments are normalized to slit 3 and added to the current slit distances. These new values of S_i are fed back into Eq. (1) and the process is iterated until the slit positions are stable.

It is known that the new drive mechanism can have periodic discrepancies arising from the rotation of the micrometer (288-step period) and motor (48-step period).[5] Sine and cosine terms of these two periods were therefore included in the dispersion function to investigate whether these discrepancies are important for the wavelength calibration. The amplitudes are estimated from the dot products of each of the terms with the data, and the procedure is included in the main iteration.

Table 2. Spectral Lines Used in the Dispersion Analyses

Lamp Type	Spectral Line (nm)	Available Slits
Cadmium (Cd)	271.2505	0–1
Mercury (Hg)	289.360	0–1
Indium (In)	293.263	0–3
Hg	296.728	0–3
Zinc (Zn)	301.836	0–5
Zn	303.578	0–5
In	303.936	0–5
Cd	313.3167	0–5
Cd	326.1055	0–5
Zn	328.233	0–5
Hg	334.148	0–5
Cd	340.3652	0–5
Cd	349.995	0–5
Cd (multiplet)	361.163	5

6. Tests of the Dispersion Function

The dispersion analysis was applied to 14 sets of spectral line data from 11 Brewer spectrometers of various types. The emission lines measured for this study are given in Table 2. Some scans were made on the multiple line of cadmium near 361 nm, which is the longest wavelength in the study. Two of the Brewers were tested at different times with different drive mechanisms. Four of the new drive mechanisms were involved in these tests, three of them operating over the full spectral range. Nine of the old-type mechanisms were involved, five of them operating over the full range. The results are given in Table 3. The amplitudes of the periodic terms are included only for the four cases when they cause a significant improvement in the fit. The slit position numbers change by less than 2 μm when the periodic terms are used and are not given separately. The rms fit is an estimate of the noise of the dispersion function, being the square root of the total squared residuals divided by the degrees of freedom. The polynomial degree used for these results was 3 for the short-scan instruments and 5 for those with the long

Table 3. Results from the New Dispersion Analysis Applied to Spectral Line Data from 11 Different Brewers (7 Double and 4 Single)[a]

Instrument Number	A288//A48 (pm)	Number of Spectral Lines	Slit Deviations (μm)					Rms Fit (pm)	Wavelength Range (nm)
			0	1	2	4	5		
119		58	−3	2	2	2	−4	5.4	56
	5.5//1.3							4.4	
119		68	5	6	7	−2	−10	3.6	70
	2.3//0.8							3.2	
145		49	9	3	2	−7	−16	2.4	60
	2.4//0.6							1.7	
009		41	19	7	14	−13	−7	3.4	42
014		20	—	16	16	−14	−24	9.3	43
017		31	16*	17	8	−7	−17	5.7	43
017		31	17*	21	12	−10	−21	2.9	43
071		17	—	14	16	−14	−25	3.8	43
	1.1//4.7							2.1	
085		23	75	52	36	−41	−69	9.3	59
100		33	13	4	15	−8	−2	13	59
107A		34	9	11	−1	−12	−16	6.9	59
107B		29	—	11	2	−11	−16	2.4	59
118		36	3	11	1	−5	−1	10	62
156		35	0	−1	−1	2	−1	3.1	59

[a]The single underlined instruments have the new grating drive, and the double underlined instruments have in addition the optimized gear. The periodicities of the micrometer and the motor are denoted A288 and A48, respectively, and are shown whenever they improved the rms fit. The rms fit is defined as the square root of the total squared residuals divided by the degrees of freedom. The last column is the wavelength range of all the spectral lines measured on slit 3. Asterisks denote narrow calibration slits.

scan. With regard to the units, a deviation of 1.0 μm in a slit position changes the wavelength by approximately 1.0 pm so that, in terms of wavelength, all the calculated numbers in Table 3 are approximately on the same scale. The last column in Table 3 shows the wavelength spread over which the dispersion function for slit 3 is valid. It is the wavelength range of all the data points on slit 3.

Table 3 is divided into three parts to facilitate comparisons between the drive mechanisms. The first part gives the results from three of the new drives operating over the full spectral range. The results in the second part are all short-scan SB's. These include results from SB 017 before and after fitting a new drive; there was no optical adjustment between these two tests. The instruments in the third part are all (long-scan) DB's with the standard drives. Two sets of data were contributed by the owner of DB 107 along with the information that the optics had been adjusted between the two tests. Results from both of these are included.

7. Results and Discussion

A. Periodic Components and the Degree of the Fitting Polynomial

The first instruments subjected to the dispersion analysis were DB 119 and 145, the first two instruments fitted with the new type of drive. As the first four lines of Table 3 show, including the periodic terms in the dispersion functions, these instruments produce definite improvement in the accuracies from 5.4 to 4.4 pm and from 2.4 to 1.7 pm. After these two drives were built, a better method was found for centering the micrometer gear wheel on the micrometer axis of rotation. Drives built by this new method were then installed in DB 119 as well as in SB 017. DB 119 was also realigned optically and equipped with the composite push rod at that time. As expected, the 288-step amplitudes for these drives are smaller than for the first new drive on DB 119, namely 2 and 2 pm versus 6 pm. The uncertainty in these estimates is approximately 1 pm.

There is only one case other than these three new-drive doubles where the fit accuracy is improved significantly by including the periodic terms. This is SB 071 in which there is a 5-pm amplitude at the motor period (48 steps). The improvement is from 3.8 pm to the extremely small value of 2.1 pm.

The phases of the periodic terms can be disturbed easily as, for example, when the micrometer is moved by hand with the drive pinion disengaged. It may therefore be preferable not to use these terms operationally even if their inclusion reduces the residual value. In this study the three instruments 119, 145, and 071 for which the periodic terms improve the fit all have quite small residuals even with the nonperiodic fit (all smaller than 4 pm since the revision of the drive of DB 119), so the choice not to include the periodic terms is quite easy.

The dispersion analysis was performed on all the data using polynomials from degree 2 up to 7. It was found that there was no improvement beyond the cubic fit for all the short-scan Brewers and for some of the DB's, including the two with the new drive. A quintic fit was the best for the remaining DB's, and, in the interest of uniformity, the results from the quintic fit are given here for all of them. It should be noted that the wavelength range over which the fits are made is not the same for all instruments.

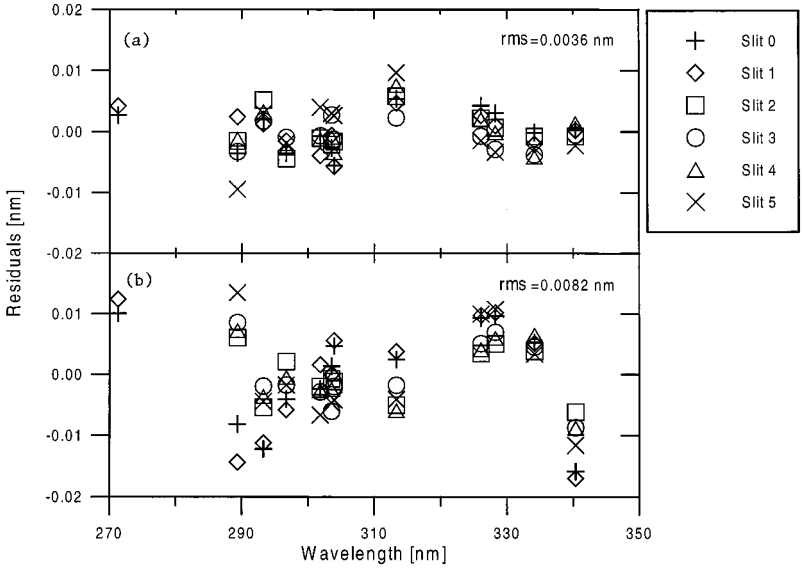

Fig. 5. Dispersion analysis results for DB 119 with the new grating drive. (a) Results from the new dispersion relation calculation using a quintic regression line and varying the slit positions to optimize the rms residuals of the fit with a total of 11 free parameters. The overall rms residuals of this analysis is 3.6 pm and uses 68 spectral line measurements. (b) The same data calculates the dispersion relation by separately fitting the data for every slit to a quadratic regression line (standard procedure). The rms residuals of this analysis is 8.2 pm.

B. Performance of the New and the Standard Dispersion Analyses

Applying the new analysis to the 14 available cases without consideration of periodicities yields rms residuals ranging from 2.4 to 13 pm with a median value of 4 pm. The larger values appear to be due to random variability in the data rather than systematic deviations that might be accommodated by different dispersion functions.

DB 119 was chosen for a comparison between the new and standard analyses because more spectral line scans were measured on this instrument than on any other and over a wider spectral range (70 nm). The standard analysis of fitting quadratic dispersion functions to the data from each slit independently yields a rms residual of 8.2 pm. The residuals are shown in the lower panel of Figure 5 whereas those of the new technique, for which the rms value is 3.6 pm, are in the upper panel. This twofold improvement is achieved with the new technique using 11 fitted parameters compared with 18 for the standard procedure.

Another aspect of the comparison can be seen in Fig. 6. This refers to slit 5 that is the slit normally used at wavelengths longer than 350 nm. It shows the points measured on slit 5 and those projected onto slit 5 from other slits by the new analysis, all relative to the new dispersion function. The curve is the standard dispersion function plotted, in the same way as the points, relative to the new function. Its main feature is the fairly rapid descent between 340 and 360 nm of nearly 0.2 nm. The longest wavelength point in Fig. 6 is from the scan on slit 5 of the 361-nm cadmium multiplet for which the equivalent line position (361.163 ± 0.015 nm) was estimated from the scan shape and the known wavelengths of the component lines. This point was not used in the derivation of either dispersion function, and it can therefore be used to compare the effectiveness of the two methods when extrapolating to 360 nm from measurements at wavelengths of 340 nm and below. The indicated errors for the standard and new methods are, respectively, 190 and 12 pm, whereas the estimated uncertainty in the equivalent line position is 15 pm rms. This example illustrates potential rather than typical errors in wavelength registration of most operating DB's because the required range of extrapolation can be reduced through use of the cadmium line at 349.995 nm. However, errors of up to 100 pm have been independently observed at long wavelengths in Brewer measurements, as already

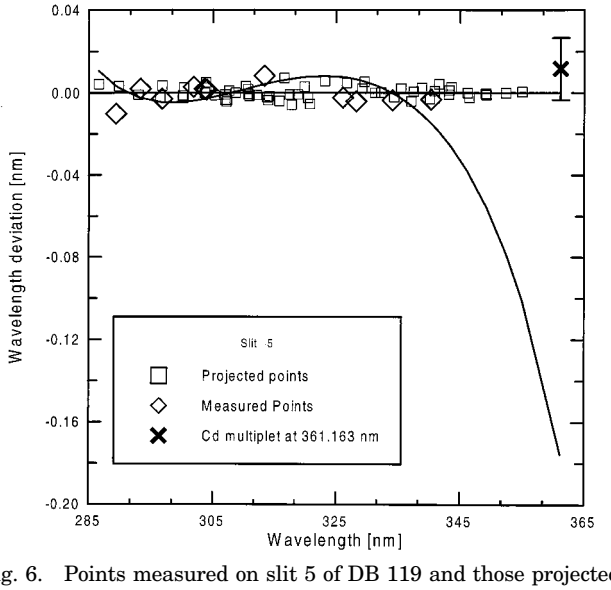

Fig. 6. Points measured on slit 5 of DB 119 and those projected onto slit 5 from other slits by the new analysis, all relative to the new dispersion function. The curve is the difference between the quadratic regression fit using only spectral lines measured on slit 5 (standard method) and the new dispersion analysis. The cadmium multiplet at 361.163 ± 0.015 nm is not used for the derivation of either dispersion function but demonstrates the different extrapolation behavior of the two dispersion functions.

noted.[7] The example shows how they can be generated by use of the standard dispersion function and much reduced by the new function.

The continuous curve in Fig. 6 is not significantly different from a straight line between 300 and 325 nm, which means that a quadratic function is adequate in this case for the restricted wavelength range. However, quadratic fits are not suitable for DB 119 beyond this range or for the whole group of long-scan instruments. The new dispersion analysis was applied to the nine cases in this group with a quadratic polynomial fit, and the average rms residual was 13.3 pm compared with 6.2 pm for the fifth-order fit, a more than twofold degradation.

C. Performance of the New and the Standard Mechanisms

Conclusions drawn from Table 3 are limited by the inhomogeneity of the data. For example, no two instruments were tested with the same set of spectral lines and, clearly, some instruments were studied much more than others. However, it is notable that three of the four new mechanisms have residuals less than 4 pm whereas only four of the ten samples of the standard drive achieve this accuracy. The average for the other six is 9.0 pm.

It is possible that the relatively poor performance of several of the standard drive mechanisms is due to wear on the contact between the micrometer and the push rod. The wire pivots in the new mechanism eliminate this source of wearing, but the micrometer itself may degrade with prolonged use. There is as yet limited data on the long-term performance of the new drive. The one in DB 119 has developed some minor faults after 10 months of trouble-free, nearly continuous use.

D. Dispersion Function and Wavelength Accuracy in Brewer UV-B Observations

In principle, the noise in the dispersion function of a particular instrument, as estimated by the rms residual of the fit, is the same as the wavelength uncertainty in irradiance measurements by that instrument. However, there is an extra wavelength shift when measurements are required at specified wavelengths, as is usually the case, because the wavelength drive can only be set to whole-number step positions. A similar step quantization is introduced by the current Hg routine that unnecessarily assigns an integer rather than a real number to the step position of the reference mercury line. An example of the combined effect of the integer steps is that a rms uncertainty of 4 pm in the dispersion function corresponds to a 5.2-pm rms variability in setting the wavelength to specified values.

Any drift in the dispersion function also contributes to the error. The current Brewer measurement routines are all based on the assumption that the dispersion function is stable except for uniform shifts in step number that can be identified by the Hg routine and compensated. This ignores the thermal stretching of the spectrum discussed above, which would change the wavelength settings around 365 nm by approximately 16 pm relative to those at 297 nm if the temperature changed by 20 °C.

8. Conclusions

A new drive to control the grating rotation of Brewer spectrometers has been developed. The thermal stability and reproducibility of the wavelength registration of a Brewer spectrometer (DB 119) fitted with the new drive mechanism have been investigated. The standard deviations of series of repeated measurements of the positions of the 297-nm mercury emission line with this instrument are less than 0.3 pm (0.04 motor steps). Based on tests with aluminum and Invar push rods, a composite push rod was made with proportions of Invar and aluminum chosen so as to minimize spectral shifts related to temperature. With this push rod, the wavelength settings change by 0.4 pm K^{-1} or less over the whole wavelength range. A spectral stretching of 1.2×10^{-5} K^{-1} has been identified.

A new method has been developed to derive the dispersion function that expresses wavelength in terms of the position in motor steps of the wavelength drive. The method uses the geometry of the Brewer spectrophotometer with its six fixed exit slits and combines spectral line measurements from all slits onto one reference slit. This new method uses 11 fitting parameters (nine on the short-scan Brewers) compared with 18 used in the standard method that fits independent quadratic functions for each of the slits. The dispersion functions that are established by the new method apply over the full range of step numbers in the line-scan data. In contrast, the functions derived by the standard method apply only to the lines measured on the particular slit, and use of these functions outside the range of calibration can generate large errors that are not present in the new method. On DB 119 with the composite push rod, the overall noise in the fit by the new method is 3.6 pm rms compared with 8.2 pm for the standard method. On slit 5 of DB 119, the standard dispersion function produces an error of 190 pm at 360 nm when derived from spectral line data measured at 340 nm and below. The corresponding error with the new method was measured as 12 ± 15 pm. The new method can reveal periodic terms in the dispersion function arising from the micrometer and motor rotations.

The new dispersion analysis has been applied to 14 sets of spectral line data from a variety of long-scan and short-scan Brewers, including four sets from Brewers with the new drive mechanism. The new mechanism has been analyzed over wavelength intervals up to 70 nm whereas the standard mechanism method has been analyzed over ranges up to 62 nm. The average rms fit for the nine long-scan cases is less than half what is achieved by quadratic fitting (6.2 versus 13.3 pm). The fits achieved by the new analysis for all 14 cases range from 2.4 to 13 pm with a median value of 4 pm. Three of the four new mechanisms exhibit rms residuals less than 4 pm whereas only four of the ten standard mechanisms achieve

this level of performance. Thus it is apparent that the new mechanisms perform comparably to the best of the standard ones, but they have not yet received comparable long-term continuous use.

Appendix A: The New Grating Drive

The new drive is shown in Fig. 1. The push rod, which transmits the motion from the micrometer to an arm mounted on the grating holder, is a 6-mm-diameter, 40-mm-long solid cylinder. It is attached at either end by short wires, 3 mm in length to the arm and 1.5 mm to the micrometer. The wires are 0.5 mm in diameter. The micrometer is of the nonrotating type (Starrett 262L) in which the spindle does not rotate as it moves backward and forward. In this application, the spindle is clamped to the monochromator frame while the thimble is rotated by a gear wheel mounted coaxially on it. The middle part of the micrometer is attached to the push rod wire and moves in response to the thimble rotation. The set screw that normally slides in a longitudinal grove in the spindle to prevent relative rotation between the middle part and the spindle is removed. Instead, the middle part is attached to the spectrometer frame by a linkage comprising two arms and two wire pivots. The linkage allows longitudinal motion, but not rotation, of the middle part. Another significant change is the elongation of the wire that sets the vertical position of the grating (this change should have been made when the wavelength range was extended from 40 to 70 nm). With the original length, the torque, which was generated in the wire by grating rotations corresponding to the extreme wavelengths, was excessive and sometimes caused the wire to twist in its mounting hole.

Substantial contributions to the design of the new wavelength drives were made by A. Ulberg, who also supervised their fabrication. T. Grajnar, V. Fioletov, and E. Wu gave valuable assistance. U. Feister, F. Kuik, K. Lamb, T. Koskela, and W. Wauben kindly provided line-scan data without which much of this study would not have been possible.

References

1. J. B. Kerr and C. T. McElroy, "Evidence for large upward trends of ultraviolet-B radiation linked to ozone depletion," Science **262,** 1032–1034 (1993).
2. C. S. Zerefos, A. F. Bais, C. Meleti, and I. C. Ziomas, "A note on the recent increase of solar UV-B radiation over northern middle latitudes," Geophys. Res. Lett. **22,** 1245–1247 (1995).
3. J. B. Kerr, C. T. McElroy, D. I. Wardle, R. A. Olafson, and W. F. J. Evans, "The automated Brewer spectrophotometer," in *Atmospheric Ozone: Proceedings of the Quadrennial Ozone Symposium*, C. S. Zereros and A. Ghazi, eds. (Reidel, Boston, Mass., 1985), pp. 396–401.
4. A. F. Bais, C. S. Zerefos, and C. T. McElroy, "Solar UVB measurements with the double- single-monochromator Brewer ozone spectrophotometer," Geophys. Res. Lett. **23,** 833–836 (1996).
5. D. I. Wardle, C. T. McElroy, J. B. Kerr, E. Wu, and K. Lamb, "Laboratory tests on the double Brewer spectrophotometer," in *Proceedings of the 1996 Quadrennial Ozone Symposium*, R. D. Bojkov and G. Visconti, eds. (Parco Scientifico e Tecnologico d'Abruzzo, Italy, 1998), pp. 997–1000.
6. F. Kuik and W. Wauben, "UV intercomparison SUSPEN," Technical Report TR-203 (Royal Netherlands Meteorological Institute, De Bilt, The Netherlands, 1998).
7. H. Slaper, H. Reinen, M. Blumthaler, M. Huber, and F. Kuik, "Comparing ground-level spectrally resolved solar UV measurements using various instruments: a technique resolving effects of wavelength shift and slit width," Geophys. Res. Lett. **22,** 2721–2724 (1995).